A Possible Second Large Subglacial Impact Crater in Northwest Greenland

MacGregor, Joseph A.; Bottke, William F., Jr.; Fahnestock, Mark A.; Harbeck, Jeremy P.; Kjaer, Kurt H.; Paden, John D.; Stillman, David E.; Studinger, Michael

Published in:
Geophysical Research Letters

DOI:
10.1029/2018GL078126

Publication date:
2019

Document version
Publisher's PDF, also known as Version of record

Geophysical Research Letters

RESEARCH LETTER
10.1029/2018GL078126

A Possible Second Large Subglacial Impact Crater in Northwest Greenland

Joseph A. MacGregor[1], William F. Bottke Jr.[2], Mark A. Fahnestock[3], Jeremy P. Harbeck[1,4], Kurt H. Kjær[5], John D. Paden[6], David E. Stillman[2], and Michael Studinger[1]

[1]Cryospheric Sciences Laboratory, NASA Goddard Space Flight Center, Greenbelt, MD, USA, [2]Department of Space Studies, Southwest Research Institute, Boulder, CO, USA, [3]Geophysical Institute, University of Alaska Fairbanks, Fairbanks, AK, USA, [4]ADNET Systems, Inc., Lanham, MD, USA, [5]Centre for GeoGenetics, Natural History Museum, University of Copenhagen, Copenhagen, Denmark, [6]Center for Remote Sensing of Ice Sheets, The University of Kansas, Lawrence, KS, USA

Abstract Following the discovery of the Hiawatha impact crater beneath the northwest margin of the Greenland Ice Sheet, we explored satellite and aerogeophysical data in search of additional such craters. Here we report the discovery of a possible second subglacial impact crater that is 36.5-km wide and 183 km southeast of the Hiawatha impact crater. Although buried by 2 km of ice, the structure's rim induces a conspicuously circular surface expression, it possesses a central uplift, and it causes a negative gravity anomaly. The existence of two closely spaced and similarly sized complex craters raises the possibility that they formed during related impact events. However, the second structure's morphology is shallower, its overlying ice is conformal and older, and such an event can be explained by chance. We conclude that the identified structure is very likely an impact crater, but it is unlikely to be a twin of the Hiawatha impact crater.

Plain Language Summary It is increasingly rare to find new large impact craters on Earth, let alone such craters buried beneath ice. We describe a possible impact crater buried beneath 2 kilometers of ice in northwest Greenland. The circular structure is more than 36 kilometers wide, and both its shape and other geophysical properties are consistent with an impact origin. If eventually confirmed as an impact crater, it would be only the second found beneath either of Earth's ice sheets. The first was the Hiawatha impact crater, which is also in northwest Greenland and only 183 kilometers away from this new structure, so we also evaluated whether these two craters could be related. They are similarly sized, but the candidate second crater appears more eroded and ice above it is much less disturbed than above the Hiawatha impact crater. Statistical analysis of the frequency of two unrelated but nearby large impacts indicates that it is improbable but not impossible that this pair is unrelated. Our study expands knowledge of the impact history of the Earth and raises the question as to how many other impact craters buried beneath ice have yet to be found.

Key Points:
- A possible second large subglacial impact crater is identified in northwest Greenland
- This crater is more than 36-km wide and is buried by more than 2 km of ice
- This crater is only 183 km from the Hiawatha impact crater but is unlikely to be a twin

Supporting Information:
- Supporting Information S1
- Data Set S1
- Movie S1
- Movie S2

Correspondence to:
J. A. MacGregor,
joseph.a.macgregor@nasa.gov

Citation:
MacGregor, J. A., Bottke, W. F., Jr., Fahnestock, M. A., Harbeck, J. P., Kjær, K. H., Paden, J. D., et al. (2019). A possible second large subglacial impact crater in northwest Greenland. *Geophysical Research Letters*, *46*, 1496–1504. https://doi.org/10.1029/2018GL078126

Received 7 JUL 2017
Accepted 5 JUN 2018
Published online 11 FEB 2019
Corrected 8 MAY 2019

This article was corrected on 8 MAY 2019. See the end of the full text for details.

1. Introduction

The geology of Earth's remote polar regions is relatively poorly known because widespread glaciation there obscures the rock surface below. Surprising discoveries continue to be made regularly regarding subglacial geology and morphology beneath polar ice sheets, which inform our understanding of past climate history and subglacial processes (e.g., Bamber, Siegert, et al., 2013; Blankenship et al., 1993; Patton et al., 2016). Of particular importance are possible subglacial impact craters, because of the potentially global effects of large impacts (Schulte et al., 2010).

The discovery of a new subaerial terrestrial impact crater greater than 6 km in diameter is considered improbable but not impossible (Hergarten & Kenkmann, 2015), while the probability of finding new subsurface craters is likely higher. The recent discovery of the subglacial Hiawatha impact crater in northwest Greenland (Kjær et al., 2018), new high-resolution maps of subglacial topography (Bamber, Griggs, et al., 2013; Fretwell et al., 2013; Morlighem et al., 2017) and the large range of subglacial erosion rates (e.g., Koppes et al., 2015) all suggest that the rarely considered possibility of large subglacial impact craters beneath either ice sheet should be revisited.

We conducted a preliminary investigation of existing satellite and aerogeophysical data sets for northwest Greenland. From that investigation, we identified one new structure that may be another subglacial impact crater and which we describe in detail in this study (Figure 1). Because of its proximity to the Hiawatha impact crater, we also evaluate the possibility that these two structures are part of a twin impact event.

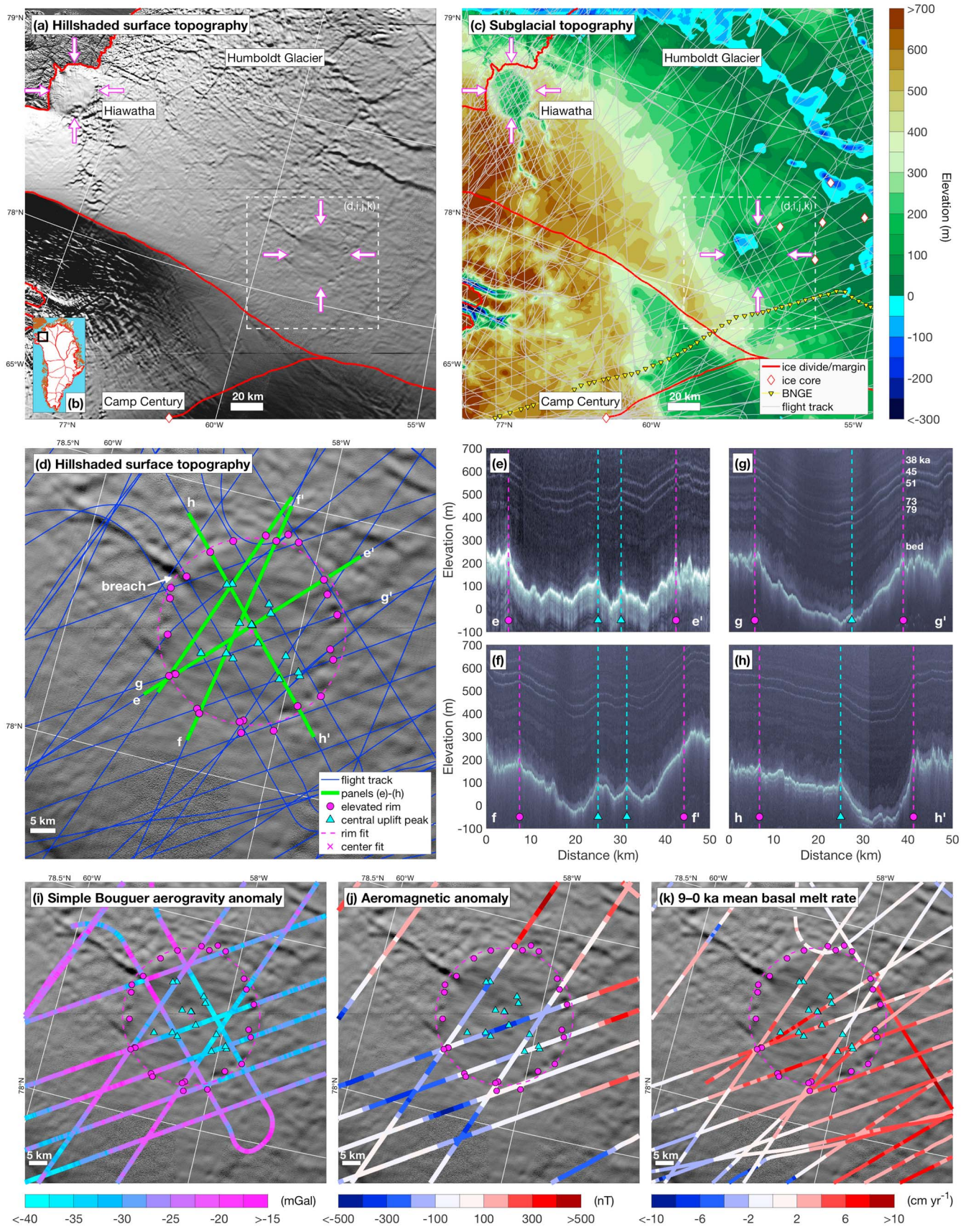
(a) Hillshaded surface topography
Humboldt Glacier
Hiawatha
(d,i,j,k)
(b)
Camp Century
20 km
79°N
78°N
65°W
77°N
60°W
55°W
(c) Subglacial topography
ice divide/margin
ice core
BNGE
flight track
>700
600
500
400
300
200
100
0
-100
-200
<-300
Elevation (m)
78.5°N
60°W
58°W
(d) Hillshaded surface topography
h
f'
e'
g'
breach
g
e
f
h'
5 km
(e)
(f)
(g)
(h)
38 ka
45
51
73
79
bed
Distance (km)
(i) Simple Bouguer aerogravity anomaly
(j) Aeromagnetic anomaly
(k) 9–0 ka mean basal melt rate
(mGal)
<-40 -35 -30 -25 -20 >-15
(nT)
<-500 -300 -100 100 300 >500
(cm yr-1)
<-10 -6 -2 2 6 >10

Table 1
Greenland Satellite and Aerogeophysical Data Sets Evaluated in This Study

Data set/instrument	Purpose	Reference[a]
ArcticDEM Release 4	Surface elevation	Polar Geospatial Center
MODIS Mosaic of Greenland	Surface texture	Haran et al. (2013)
BedMachine v3	Subglacial topography	Morlighem et al. (2017) and Kjær et al. (2018)
Airborne Topographic Mapper	Ssurface slope	Studinger (2017)
Multi-Channel Coherent Radar Depth Sounder	Subglacial topography and internal structure	Leuschen (2018)
Radiostratigraphy of the Greenland Ice Sheet	Age structure	MacGregor et al. (2015)
Holocene ice flow of the Greenland Ice Sheet	Holocene vertical strain rate	MacGregor, Colgan, et al. (2016)
Basal thermal state of the Greenland Ice Sheet	Likely basal thermal state and melt rate	MacGregor, Fahnestock, et al. (2016)
Sander AIRGrav gravimeter	Gravity anomaly	Cochran and Bell (2016)
LDEO gravimeter	Gravity anomaly	Tinto (2018)
Scintrex CS-3 cesium magnetometer	Magnetic anomaly	Cochran et al. (2014)

[a]Instrument and data set precision, accuracy and spatiotemporal resolution discussed therein.

2. Data and Methods

2.1. Morphology and Geology

We primarily evaluate 11 Greenland-specific remote sensing data sets in this study (Table 1). One data set is derived from commercial satellite imagery (ArcticDEM), and the remaining nine are derived from National Aeronautics and Space Administration (NASA) satellite imagery and 25 years of NASA aerogeophysical surveys of the Greenland Ice Sheet (1993–2017).

Four of these 10 data sets are gridded and provide regional context for the structure. The first gridded data set is ArcticDEM, which is a high-resolution elevation model of the subaerial ice sheet surface and allows us to detect subtle changes in surface slope that are not otherwise apparent in visible imagery. The Moderate Resolution Imaging Spectroradiometer (MODIS) Mosaic of Greenland (MOG) provides a similar perspective, as it represents a high-pass-filtered view of the ice sheet surface (e.g., Bell et al., 2006; MacGregor, Fahnestock, et al., 2016; Scambos et al., 2007). The third gridded data set is the subglacial topography. In our region of interest, this topography is derived from both ordinary kriging of radar-measured ice thickness in the ice sheet interior (including over the new structure) and mass conservation closer to the ice margin where the ice flows more quickly, including over the Hiawatha impact crater (Morlighem et al., 2017). The fourth gridded data set is the likely basal thermal state of the ice sheet, which is a synthesis of multiple remote sensing data sets and ice sheet models. The remaining seven data sets include high-resolution along-track information regarding local surface slope, englacial age structure, past ice flow, subglacial topography, and geology. These data sets are generally used as is, except for the aerogravity data sets. Following Studinger (1998) and assuming an ice density of 917 kg m^{-3} and a crustal density of 2,670 kg m^{-3}, we correct the free-air gravity anomaly to a simple Bouguer slab anomaly that accounts for spatially variable ice thickness and subglacial topography.

Following Kjær et al. (2018), we identify the location of possible elevated rims and peaks in the central uplift, which are characteristic features of complex craters (e.g., Melosh, 1989), by examining the bed reflection in airborne radar-sounding profiles collected over the structure. We then project the rim picks onto a local polar

Figure 1. (a) Hillshaded ArcticDEM surface elevation across northwestern Greenland, showing both the Hiawatha impact crater along the ice margin and the presently identified structure farther inland to the southeast. Horizontal lines across the panel are mosaicking artifacts. Magenta arrows indicate location of both structures. Ice divides and margin are from Zwally et al. (2012) and Howat et al. (2014), respectively. Locations of 1953–1954 British North Greenland Expedition (BNGE) traverse stations, 1959–1967 Camp Century station, and 1995 Humboldt Glacier shallow ice core sites are from Paterson (1955), Colgan et al. (2016) and Mosley-Thompson et al. (2001), respectively. Location of panels (d), (i), (j), and (k), supporting information Figure S1 and Movies S1 and S2, shown as white dashed box. (b) Map of Greenland with black box showing location of panels (a) and (c). (c) Gridded subglacial topography across northwestern Greenland (Morlighem et al., 2017; Kjær et al., 2018). The 1993–2017 NASA and 2016 Alfred Wegener Institute (AWI) flight tracks are from Leuschen (2018) and Kjær et al. (2018), respectively. (d) Hillshaded ArcticDEM in the vicinity of possible second impact crater, with overlain radar-identified features (elevated rim and peaks in central uplift) and best fit circle to rim identifications. A breach in the western portion of the rim is highlighted. (e–h) Selected radargrams over the possible impact crater from 14 May 1999, 5 May 2014, 16 May 2012, and 17 April 2017, respectively. Vertical dashed lines indicate identified elevated rim and peaks in the central uplift. In (g), the ages of five prominent deep reflections (MacGregor et al., 2015), and the ice bed reflection are identified. (i) Simple Bouguer aerogravity anomaly, (j) aeromagnetic anomaly (not reduced to pole), and (k) 9- to 0-ka mean basal melt rate over the second possible impact crater (Table 1).

Table 2
Key Properties of Subglacial Impact Craters in Northwest Greenland

		Subglacial impact crater	
Property	Units	Hiawatha	*Paterson*[a]
Center latitude	°N	78.72	78.27
Center longitude	°W	66.33	58.41
Diameter	km	31.1 ± 0.3	36.5 ± 0.2
Rim-to-floor depth	m	320 ± 70	160 ± 100
Depth-to-diameter ratio		0.010 ± 0.002	0.004 ± 0.003
Maximum central peak width	km	8	23
Maximum central peak subglacial relief	m	50	100
Maximum thickness of overlying ice	m	950	2,180
Minimum age of overlying ice	ka	12.8	79
Reference		Kjær et al. (2018)	This study

[a]Suggested name for the structure described in this study is discussed in section 5.

stereographic projection centered on the structure and perform a linear regression that assumes a circular fit to these picks. This best fit circle and its center provide context for the interpretation of all other data sets.

2.2. Impact Frequency

The frequency of impacts that generate large terrestrial craters has been estimated in different ways (hereafter simply *large impact rate*, where *large* signifies >20-km diameter). For example, Hughes (2000) estimated an approximate large impact rate of 3×10^{-15} km^{-2} yr^{-1} over the past 125 ± 20 Myr based on confirmed craters that formed within the North American, European, and Australian cratons. Using new methods to date lunar craters and hence to constrain lunar and terrestrial impact rates, Mazrouei et al. (2019) inferred that ~355 ± 90 large terrestrial craters formed over the last 650 Myr. This total is equivalent to a large impact rate of $1.0 \pm 0.3 \times 10^{-15}$ km^{-2} yr^{-1}, though that value may have increased to between 2.5 and 2.8 (±1.1) $\times 10^{-15}$ km^{-2} yr^{-1} over the last ~100 Myr. Of the 41 confirmed large terrestrial craters, 38 are younger than 650 Ma (Earth Impact Database, 2017; Mazrouei et al., 2019). We use these values as benchmarks to determine the probability that Hiawatha impact crater and the second structure identified in this study formed in such proximity by chance.

We use two separate methods to calculate the frequency of an impact crater of the structure's size and the likelihood of two such nearby craters being part of the same event. Both methods use Monte Carlo algorithms (e.g., Bottke & Andrews-Hanna, 2017). The first method uses conventional estimates of crater production rates (Hughes, 2000), whereas the second method leverages the lunar impact rate to infer the terrestrial impact rate and hence the recurrence interval of large impacts (Mazrouei et al., 2019). The second method is similar to the well-known *birthday problem*, involving the calculation of the probability that, from a randomly chosen population, a pair thereof will have the same birthday. This probability becomes surprisingly high for relatively small populations, for example, >50% for 23 people. Here we evaluate the likelihood that a pair of craters is separated less than a given distance merely by chance, that is, that they do not share a birthday.

3. Results

3.1. Morphology and Geology

From the subglacial topography of 13 distinct flight segments over the structure between 1997 and 2017, we identified 26 candidate crossings of an elevated rim and 15 candidate peaks of a central uplift (Figures 1d–1h and supporting information Movie S1 and Data Set S1). Conservatively, assuming a positional uncertainty of 1 km for the rim picks, the best fit diameter of this possible crater is 36.5 ± 0.2 km. This circle encloses a subglacial basin that is covered by up to 2,180 m of ice. The best fit center of this structure is 183 km southeast (102°) of the center of the Hiawatha impact crater, and the mean rim-to-floor depth is 160 ± 100 m. The central peaks are elevated up to 100 m from the structure's floor, and they are separated by up to 23 km from each other. The depth-to-diameter ratio is 0.004 ± 0.003. This value is less than half that for the Hiawatha impact crater (0.010 ± 0.002), and both are unusually low compared to subaerial complex craters (≤0.2; Melosh, 1989). These key properties of both hypothesized subglacial impact craters are summarized in Table 2.

Neither the rim nor the central uplift are well resolved by the 150-m gridded subglacial topography, which is likely due to the geostatistical compromises inherent in gridding bed topography from radar sounding across an entire ice sheet. While the circular shape of the structure is less distinct than that of the Hiawatha impact crater, the latter was surveyed more densely by radar sounding in 2016. The present radar coverage of the structure is broadly similar to that of the Hiawatha impact crater prior to 2016.

When these radar identifications are overlain on a hillshaded ArcticDEM and MOG, the circular surface expression of the relatively flat subglacial structure is clear (Figure 1d and Movie S2). Although this surface expression is subtler than that of the Hiawatha impact crater (Figure 1a), the best fit circle clearly follows surface slopes inferred from the hillshaded ArcticDEM and derived from airborne laser altimetry (Figures 1a and 1d and Movie S2). ArcticDEM also suggests a breach that crosscuts the western rim and a

subglacial trough that continues several tens of kilometers downstream. Immediately downstream of this apparent breach, the subglacial trough is >300-m deep with a width-to-height ratio of ~6–10 (Movie S1), suggesting that it formed subglacially (Livingstone et al., 2017). Northeast of the structure, two larger and deeper east/west trending troughs are similarly resolved by ArcticDEM, MOG, and radar sounding, supporting our interpretation of the presence of a trough (Figures 1a and 1c; Livingstone et al., 2017).

Available aerogravity and aeromagnetic data are sparser than other airborne data sets (Figures 1i and 1j). The aerogravity data indicate an off-center negative Bouguer anomaly within the structure whose magnitude (>15 mGal) is consistent with that expected for a buried impact crater of the structure's size (Pilkington & Grieve, 1992). The aeromagnetic anomaly over the structure is also mostly negative, and its magnitude is largest (<−300 nT) near the center of the structure, but this observation is less significant as such anomalies are known to vary significantly over impact craters (Pilkington & Grieve, 1992).

3.2. Preliminary Age Constraint

Based on the dated radiostratigraphy of the Greenland Ice Sheet, available for pre-2014 radar data only, the ice overlying the structure is at least 79 ka old (Figures 1e–1h; MacGregor et al., 2015). These reflections were dated using the depth-age relationships from six deep (>1 km) ice cores, including two cores within 200 km of the structure and vertical ice flow modeling of the ages of reflections not observed at ice core sites. The five shallow (<150 m) ice cores on Humboldt Glacier within 75 km of the structure's center were not included in this reflection dating (Figure 1c). The shallowest three of the five dated reflections identified in Figure 1g are commonly observed across the Greenland Ice Sheet and their ages are relatively well constrained (38–51 ka; MacGregor et al., 2015). These reflections are clearly conformal with each other, drape smoothly over the bed and appear generally undisturbed. This englacial age structure contrasts significantly with that of the ice overlying the Hiawatha impact crater, for which no conformal ice is unambiguously older than the beginning of the Younger Dryas at 12.8 ka and whose basal ice is heavily disturbed (Kjær et al., 2018).

The period necessary to erode a putative crater to its present morphology also loosely constrains its age (Kjær et al., 2018). Subglacial erosion rates vary significantly, between 10^{-5} and 10^{-2} m yr^{-1}, and this rate depends on several factors, including the thermal state at the base of the ice sheet (e.g., Cowton et al., 2012; Koppes et al., 2015). Assuming that the structure's original morphology had a rim-to-floor depth of >1 km, which is consistent with that expected for a crater of this size (Collins et al., 2005) but an order of magnitude greater than its present value (~160 m), then $>10^5$ years is required to erode into the present morphology beneath a thawed ice sheet bed and $>10^8$ years for a frozen bed. This simple calculation ignores likely subglacial sediment deposition on the crater floor, which would occur at a rate comparable to erosion and decrease the burial period.

3.3. Impact Frequency

If we assume that the large impact rate is 3×10^{-15} km^{-2} yr^{-1} (Hughes, 2000), that the crater-to-projectile diameter ratio is ~20 for Earth-impacting projectiles traveling at 20 km s^{-1} (Bottke et al., 2002; Melosh, 1989), and that these projectiles follow the size-frequency distribution of near-Earth objects (Harris & D'Abramo, 2015), we find that 36.5-km-wide craters form at rates ~3.2 times lower than for all large craters. This value implies a recurrence interval of ~2.1 Myr. For Hiawatha-sized craters of 31.1 km, this production rate is only ~2.3 times larger, so the recurrence interval is slightly smaller (1.5 Myr). We find that for every million synthetic large craters produced on Earth, ~210 such craters will fall within 183 km of each other. If we further assume a single 36.5-km-wide crater has already formed, the probability that a large crater of any size will form within a 183-km radius around it is 2.1×10^{-4}, that is, the ratio of that surface area to that of the whole Earth. Given that the recurrence interval of 31.1-km craters is 1.5 Myr, the above probability implies that an unrelated large crater pair of the observed proximity should occur every 7.1 Gyr.

For the birthday problem, we consider the probability that in a set of 355 ± 90 randomly chosen large craters that formed since 650 Ma (Mazrouei et al., 2019) some crater pairs will form within our threshold distance (183 km) on stable terrain, so that the crater pair persists until the present. For each of 1,000 iterations of a Monte Carlo algorithm, we randomly chose the location of 355 large terrestrial craters and determined the separation distances between all possible pairs. Following this method, we find that on average 13 large crater pairs are separated by less than 183 km. Mazrouei et al. (2019) estimated that 10.7 ± 3.1% of the Earth's surface was stable enough to possess craters as old as 650 Ma by taking the ratio of the number of known large terrestrial craters (38) to the number inferred to have been produced during that period from

the lunar production rate (355). We argue that this estimate is reasonable because large lunar and terrestrial craters formed over the last 650 Myr have both a similarly shaped size-frequency distribution and a similar age distribution, but this argument holds only if crater erasure mechanisms on stable terrestrial terrain are less pronounced than previously thought. The product of the predicted number of unrelated proximal crater pairs (13) and the fraction of stable terrestrial terrain (10.7 ± 3.1%) suggests that the number of large unrelated crater pairs separated by less than 183 km on stable terrestrial terrain is one or two (1.4 ± 0.4).

4. Discussion

Here we consider two key questions regarding the identified structure. First, is this structure an impact crater? If so, then what is its relationship (if any) to the Hiawatha impact crater?

Although the structure is unusually shallow for a complex crater, the circular surface expression, the consistently elevated rim, flat floor and the presence of a central uplift are all morphologically consistent with a complex crater. The radar-identified peaks in the central uplift are sufficiently separated (up to 23 km apart or ~64% of the structure's diameter) that we speculate that they form a nascent central peak ring, consistent with the expected morphology for such a structure (Melosh, 1989). For subaerial complex craters on Earth, the gradational transition from a central peak to a central peak ring is predicted to occur at a diameter of $<$25 km (Melosh, 1989), so the presence of a central peak ring within the structure is plausible. The negative aerogravity anomaly within the structure's perimeter is also consistent with an impact crater, but these data are sparse enough that it is not yet clear if the anomaly is concentric within the structure, and anomalies of a similar magnitude are observed ~40 km southwest of the structure's rim. The negative aeromagnetic anomaly within the structure's perimeter somewhat challenges an impact origin for the structure. However, this anomaly could be due to nonmagnetic postimpact sedimentary fill, which could also account for the muted crater morphology (Pilkington & Grieve, 1992).

Volcanic or periglacial processes can also sometimes produce quasi-circular morphologies (e.g., calderas or cirques, respectively), but they are not necessarily circular nor must they possess a central uplift. Most of Greenland's bedrock is likely Precambrian in age ($>$541 Ma; Dawes, 2009), but active subglacial volcanism has been identified in part of northeastern Greenland (Fahnestock et al., 2001). Critically, neither the negative aerogravity nor the negative aeromagnetic anomalies observed over the structure are consistent with a volcanic origin (Blankenship et al., 1993). Based on the sum of the available observations, we conclude that the structure is very likely an impact crater.

Twin or multiple large terrestrial craters may exist because ~15% of near-Earth asteroids are binaries or multiples (Bottke Jr. & Melosh, 1996; Margot et al., 2015; Walsh & Jacobson, 2015). Dynamical modeling suggests that most binaries form when nongravitational forces spin asteroids up fast enough for them to shed mass (Walsh & Jacobson, 2015; Walsh et al., 2008). Other binary asteroids may form when smaller celestial bodies undergo tidal disruption near large terrestrial planets (e.g., Bottke & Melosh, 1996). The discovery of two closely spaced, similarly sized complex craters thus requires an initial evaluation of the twin hypothesis, that is, that they formed near simultaneously.

Observations that favor the twin hypothesis include the proximity and size of both structures, their similar morphologies, the local ice flow history, and apparent local basal melting. Beneath the structure itself, the basal thermal state is identified as being likely thawed presently (MacGregor, Fahnestock, et al., 2016), which is also supported by a prior analysis of bed reflectivity there (Oswald & Gogineni, 2012). Based on our simple erosion period estimates (~10^5–10^8 years), this present basal thermal state suggests that the structure is unlikely to be older than the Pleistocene (2.6 Ma–11.7 ka), during which time a large ice sheet waxed and waned over Greenland (Bierman et al., 2016; Schaefer et al., 2016). Evidence of basal melting and past rapid ice flow in this region during part of the Holocene (9 ka to present) suggests that ice flow over the structure is anomalous (Figure 1k and Movie S2; MacGregor, Colgan, et al., 2016; MacGregor, Fahnestock, et al., 2016), but this pattern could instead be related to the event that produced the more likely geologically recent Hiawatha impact crater, not this second structure. An impact into thicker ice above this structure during the Pleistocene, as compared to over the Hiawatha impact crater (Peltier et al., 2015), would have further dampened the final crater morphology (Senft & Stewart, 2008), and this thicker ice would also have had greater driving stress, leading it to more quickly override and bury the resulting crater. Further, the structure does not appear to be a significant hydropotential low presently, suggesting that any subglacial water present may be generated locally.

Observations that disfavor the twin hypothesis include the radiostratigraphic conformability and age of the overlying ice, lack of evidence of ongoing subglacial erosion, other formerly subglacial impact craters, and uncertainty regarding the past history of the Greenland Ice Sheet. Given the conformable age structure of the overlying ice, a twin event would require that the ice sheet rapidly override the structure and thermodynamically equilibrate with impact-generated heat sources since the late Last Glacial Period, the youngest possible age of the Hiawatha impact structure (Kjær et al., 2018). No ice flow modeling has yet been performed to evaluate this possibility, but it appears improbable. Modeling of subaerial impacts on Mars suggests that a hydrothermal system would likely still exist following such a short postimpact period (Abramov & Kring, 2005). From airborne radar sounding, such a system may be present beneath the Hiawatha impact crater (Kjær et al., 2018), but there is not yet such evidence beneath this second structure. Further, radar reflectivity patterns suggest that the basal ice directly overlying the Hiawatha impact crater is debris rich, and much of this debris clearly originates at the bed, indicating active subglacial erosion. No such radar signature clearly exists within the basal ice above the second crater (Figures 1e–1h). Additionally, multiple terrestrial craters elsewhere have been recently covered by ice for potentially extended periods (~10^5–10^6 yr), and yet they partly retain their topographic expression, for example, the Clearwater Lake craters in Québec, Canada (Schmieder et al., 2015). Finally, the present basal thermal state could easily have varied in the past, and this state is particularly difficult to constrain for this sector of the Greenland Ice Sheet (Aschwanden et al., 2016).

The first of the two methods we used to evaluate impact frequency indicates a recurrence interval for nearby craters of these sizes (7.1 Gyr) that is greater than the age of the Earth, implying that the craters' proximity is unlikely to be a matter of chance and favoring the twin hypothesis. However, the second method, that is, the birthday problem calculation, indicates that one or two such pairs should exist on Earth presently. Two large unrelated crater pairs are already known: (1) The Boltysh (24 km) and Obolon' (20 km) craters in Ukraine, which are separated by 108 km yet were formed 104 Myr apart (Earth Impact Database, 2017); and (2) The overlapping Clearwater Lake craters in Canada, which are ~26 and ≥36 km in diameter and separated by ~30 km yet differ in age by ~180 Myr (Schmieder et al., 2015). Considering the uncertainty (90, or 25%) in the number of large terrestrial craters (355) predicted by Mazrouei et al. (2019), two such pairs are certainly plausible, while three is less likely. We note that our Monte Carlo modeling predicts that only the East and West Clearwater Lake crater pair is a low-probability event (~5–10% in the past 650 Myr). Further, no nearly equal size binary asteroids in the near-Earth asteroid population have yet been discovered (Johnston, 2017), suggesting a dearth of suitable impactors to explain similar-size crater pairs. Models of their formation suggest that they are difficult to form or keep stable by rotational fission (e.g., Jacobson & Scheeres, 2011). Hence, while it less surprising that the Hiawatha pair could be unrelated than for the Clearwater Lake or Ukrainian pairs, the scenario that all three crater pairs are unrelated is broadly consistent with our present understanding of impact frequency and impactor populations.

5. Conclusions

We presented aerogeophysical evidence for a second large (>36 km) subglacial impact crater with a possible nascent central peak ring in northwestern Greenland. While conclusive identification of this structure as an impact crater awaits further research, including direct sampling (French & Koeberl, 2010), this new structure is potentially the 22nd largest terrestrial impact crater (Earth Impact Database, 2017). The possibility of additional subglacial craters beneath the Greenland and Antarctic ice sheets should be investigated, as our discovery further emphasizes the ability of ice sheets to both bury and preserve evidence of terrestrial impacts.

This hypothesized subglacial impact crater is 183 km southeast of the Hiawatha impact crater. This crater pair possesses several similarities (circular surface expression, elevated rim, central uplift, and size), but other englacial and subglacial characteristics are divergent (ice age, depth-to-diameter ratio, and basal ice), and their proximity is plausibly but not conclusively explained by chance. So, based on presently available data and our modeling, we assess that this second crater is unlikely to be part of a twin impact event with the Hiawatha impact crater. Such an event would be a rare occurrence on Earth for confirmed or unconfirmed impact craters.

Besides Humboldt Glacier and five shallow ice cores collected nearby in 1995 (the Humboldt cores, Figure 1c), there are no named geographic features overlying the structure we identified in this study (Bjørk et al., 2015). The earliest known ground-based investigation of this region is the 1953–1954 British North Greenland

Expedition (Figure 1c), which included eminent glaciologist W. S. B. (Stan) Paterson (Paterson, 1955). Should the impact origin of this structure be established definitively, we suggest respectfully that it be named the Paterson crater.

Acknowledgments
We thank NASA's Program for Arctic Regional Climate Assessment (PARCA), Operation IceBridge and Scientific Visualization Studio for incidental data collection over the identified structure, unrestricted data distribution and visualization thereof, respectively. We thank the National Snow and Ice Data Center (NSIDC) for data archiving and accessibility. Except for ArcticDEM, all investigated data sets are archived and freely available at NSIDC. ArcticDEM was created by the Polar Geospatial Center (PGC) from DigitalGlobe, Inc. imagery and is archived and freely available by PGC. We thank L. C. Andrews, A. A. Bjørk, G. K. C. Clarke, W. T. Colgan, K. Cuffey, R. E. Grimm, M. Morlighem, K. E. Poinar, E. D. Waddington, and the Greenland Language Secretariat for valuable discussions, the Editor, and four anonymous referees for constructive reviews. W. F. B.'s participation was supported by NASA's SSERVI program, *Institute of the Science of Exploration Targets (ISET)*, institute grant NNA14AB03A.

References

Abramov, O., & Kring, D. A. (2005). Impact-induced hydrothermal activity on early Mars. *Journal of Geophysical Research*, *110*, E12S09. https://doi.org/10.1029/2005JE002453

Aschwanden, A., Fahnestock, M. A., & Truffer, M. (2016). Complex Greenland outlet glacier flow captured. *Nature Communications*, *7*, 10524. https://doi.org/10.1038/ncomms10524

Bamber, J. L., Griggs, J. A., Hurkmans, R. T. W. L., Dowdeswell, J. A., Gogineni, S. P., Howat, I., et al. (2013). A new bed elevation dataset for Greenland. *The Cryosphere*, *7*(2), 499–510. https://doi.org/10.5194/tc-7-499-2013

Bamber, J. L., Siegert, M. J., Griggs, J., Marshall, S. J., & Spada, G. (2013). Paleofluvial mega-canyon beneath the central Greenland ice sheet. *Science*, *341*(6149), 997–999. https://doi.org/10.101126/science.1239794

Bell, R. E., Studinger, M., Fahnestock, M. A., & Shuman, C. A. (2006). Tectonically controlled subglacial lakes on the flanks of the Gamburtsev Subglacial Mountains, East Antarctica. *Geophysical Research Letters*, *33*, L02504. https://doi.org/10.1029/2005GL025207

Bierman, P. R., Shakun, J. D., Corbett, L. B., Zimmerman, S. R., & Rood, D. H. (2016). A persistent and dynamic East Greenland ice sheet over the past 7.5 million years. *Nature*, *540*(7632), 256–260. https://doi.org/10.1038/nature20147

Bjørk, A. A., Kruse, L. M., & Michaelsen, P. B. (2015). Brief communication: Getting Greenland's glaciers right—A new data set of all official Greenlandic names. *The Cryosphere*, *9*(6), 2215–2218. https://doi.org/10.5194/tc-9-2215-2015

Blankenship, D. D., Bell, R. E., Hodge, S. M., Brozena, J. M., Behrendt, J. C., & Finn, C. A. (1993). Active volcanism beneath the West Antarctic ice sheet and implications for ice-sheet stability. *Nature*, *361*(6412), 526–529. https://doi.org/10.1038/361526a0

Bottke, W. F. Jr., & Melosh, H. J. (1996). Binary asteroids and the formation of doublet craters. *Icarus*, *124*(2), 372–391. https://doi.org/10.1006/icar.1996.0215

Bottke, W. F., & Andrews-Hanna, J. (2017). A post-accretionary lull in large impacts on early Mars. *Nature Geoscience*, *10*(5), 344–348.

Bottke, W. F., Morbidelli, A., Jedicke, R., Petit, J.-M., Levison, H., Michel, P., & Metcalfe, T. S. (2002). Debiased orbital and size distributions of the near-Earth objects. *Icarus*, *156*(2), 399–433. https://doi.org/10.1006/icar.2001.6788

Cochran, J. R., & Bell, R. E. (2016). IceBridge Sander AIRGrav L1B geolocated free air gravity anomalies, version 1, NASA National Snow and Ice Data Center Distributed Active Archive Center, Boulder, Colorado, USA. https://doi.org/10.5067/R1RQ6NRIJV89 [Accessed 11 January 2017].

Cochran, J. R., Burton, B., Frearson, N., & Tinto, K. (2014). IceBridge Scintrex CS-3 cesium magnetometer L1B geolocated magnetic anomalies, version 2, NASA National Snow and Ice Data Center Distributed Active Archive Center, Boulder, Colorado, https://doi.org/10.5067/OY7C2Y61YSYW [Accessed 11 January 2017].

Colgan, W., Machguth, H., MacFerrin, M., Colgan, J. D., van As, D., & MacGregor, J. A. (2016). The abandoned ice sheet base at Camp Century, Greenland, in a warming climate. *Geophysical Research Letters*, *43*, 8091–8096. https://doi.org/10.1002/2016GL069688

Collins, G. S., Melosh, H. J., & Marcus, R. A. (2005). Earth impact effects program: A web-based computer program for calculating the regional environmental consequences of a meteoroid impact on Earth. *Meteoritics and Planetary Science*, *40*(6), 817–840. https://doi.org/10.1111/j.1945-5100.2005.tb00157.x

Cowton, T., Nienow, P., Bartholomew, I., Sole, A., & Mair, D. (2012). Rapid erosion beneath the Greenland ice sheet. *Geology*, *40*(4), 343–346. https://doi.org/10.1130/G32687.1

Dawes, P. R. (2009). The bedrock geology under the inland ice: The next major challenge for Greenland mapping. *Geological Survey of Greenland and Denmark Bulletin*, *17*, 57–60.

Earth Impact Database (2017). http://www.passc.net/EarthImpactDatabase/index.html. [Accessed 11 January 2017].

Fahnestock, M., Abdalati, W., Joughin, I., Brozena, J., & Gogineni, P. (2001). High geothermal heat flow, basal melt, and the origin of the rapid ice flow in central Greenland. *Science*, *294*(5550), 2338–2342. https://doi.org/10.1126/science.1065370

French, B. M., & Koeberl, C. (2010). The convincing identification of terrestrial meteorite impact structures: What works, what doesn't, and why. *Earth Science Reviews*, *98*(1-2), 123–170. https://doi.org/10.1016/j.earscirev.2009.10.009

Fretwell, P. J., Pritchard, H. D., Vaughan, D. G., Bamber, J. L., Barrand, N. E., Bell, R. E., et al. (2013). Bedmap2: Improved ice bed, surface and thickness datasets for Antarctica. *The Cryosphere*, *7*(1), 375–393. https://doi.org/10.5194/tc-7-375-2015

Haran, T., Bohlander, J., Scambos, T., Painter, T., & Fahnestock, M. (2013). MEaSUREs MODIS Mosaic of Greenland 2005 (MOG2005) Image Map, Version 1. NASA National Snow and Ice Data Center Distributed Active Archive Center, Boulder, Colorado. 10.5067/IAGYM8Q26QRE [Accessed 11 January 2017].

Harris, A. W., & D'Abramo, G. (2015). The population of near-Earth asteroids. *Icarus*, *257*, 302–312. https://doi.org/10.1016/j.icarus.2015.05.004

Hergarten, S., & Kenkmann, T. (2015). The number of impact craters on Earth: Any room for further discoveries? *Earth and Planetary Science Letters*, *425*, 187–192. https://doi.org/10.1016/j.epsl.2015.06.009

Howat, I. M., Negrete, A., & Smith, B. E. (2014). The Greenland Ice Mapping Project (GIMP) land classification and surface elevation data sets. *The Cryosphere*, *8*(4), 1509–1518. https://doi.org/10.5194/tc-8-1509-2014

Hughes, D. W. (2000). A new approach to the calculation of the cratering rate of the Earth over the last 125 20 Myr. *Monthly Notices of the Royal Astronomical Society*, *317*, 429–437.

Jacobson, S. A., & Scheeres, D. J. (2011). Dynamics of rotationally fissioned asteroids: Source of observed small asteroid systems. *Icarus*, *214*(1), 161–178. https://doi.org/10.1016/j.icarus.2011.04.009

Johnston, R. J. (2017). Asteroids with satellites. http://www.johnstonsarchive.net/astro/asteroidmoons.html. [Accessed 19 May 2017].

Kjær, K. H., Larsen, N. K., Binder, T., Bjørk, A. A., Eisen, O., Fahnestock, M. A., et al. (2018). A large impact crater beneath Hiawatha Glacier in northwest Greenland. *Science Advances*, *4*(11), eaar8173-12. https://doi.org/10.1126/sciadv.aar8173

Koppes, M., Hallet, B., Rignot, E., Mouginot, J., Smith Wellner, J., & Boldt, K. (2015). Observed latitudinal variations in erosion as a function of glacier dynamics. *Nature*, *526*(7571), 100–103. https://doi.org/10.1038/nature15385

Leuschen, C. (2018). IceBridge MCoRDS L1B geolocated radar echo strength profiles, version 2. NASA National Snow and Ice Data Center Distributed Active Archive Center. https://doi.org/10.5067/90S1XZRBAX5N [Accessed 18 May 2018]

Livingstone, S. J., Chu, W., Ely, J. C., & Kingslake, J. (2017). Paleofluvial and subglacial channel networks beneath Humboldt Glacier, Greenland. *Geology*, *45*(6), 551–554. https://doi.org/10.1130/G38860.1

MacGregor, J. A., Colgan, W. T., Fahnestock, M. A., Morlighem, M., Catania, G. A., Paden, J. D., & Gogineni, S. P. (2016). Holocene deceleration of the Greenland ice sheet. *Science*, *351*(6273), 590–593. https://doi.org/10.1126/science.aab1702

MacGregor, J. A., Fahnestock, M. A., Catania, G. A., Aschwanden, A., Clow, G. D., Colgan, W. T., et al. (2016). A synthesis of the basal thermal state of the Greenland ice sheet. *Journal of Geophysical Research: Earth Surface*, *121*, 1328–1350. https://doi.org/10.1002/2015JF003803

MacGregor, J. A., Fahnestock, M. A., Catania, G. A., Paden, J. D., Gogineni, S. P., Young, S. K., et al. (2015). Radiostratigraphy and age structure of the Greenland ice sheet. *Journal of Geophysical Research: Earth Surface*, *120*, 212–241. https://doi.org/10.1002/2014JF003215

Margot, J.-L., Pravec, P., Taylor, P., Carry, B., & Jacobson, S. (2015). Asteroid systems: Binaries, triples, and pairs. In P. Michel, F. DeMeo, & W. F. Bottke (Eds.), *Asteroids IV*, (pp. 355–374). Tucson, AZ: U. Arizona Press. https://doi.org/10.2458/azu_uapress_9780816532131-ch019

Mazrouei, S., Ghent, R. R., Bottke, W. F., Parker, A. H., & Gernon, T. M. (2019). Earth and Moon impact flux increased at the end of the Paleozoic. *Science*, *363*(6424), 253–257. https://doi.org/10.1126/science.aar4058

Melosh, H. J. (1989). Impact cratering: A geologic process. *Oxford Monographs on Geology and Geophysics*, *11*, 245.

Morlighem, M., Williams, C. N., Rignot, E., An, L., Arndt, J., Bamber, J. L., et al. (2017). BedMachine v3: Complete bed topography and ocean bathymetry mapping of Greenland from multi-beam echo sounding combined with mass conservation. *Geophysical Research Letters*, *44*, 11,051–11,061. https://doi.org/10.1002/2017GL074954

Mosley-Thompson, E., McConnell, J. R., Bales, R. C., Li, Z., Lin, P., Steffen, K., et al. (2001). Local to regional-scale variability of annual net accumulation on the Greenland ice sheet from PARCA cores. *Journal of Geophysical Research*, *106*(D24), 33,839–33,851. https://doi.org/10.1029/2001JD900067

Oswald, G. K. A., & Gogineni, S. P. (2012). Mapping basal melt under the northern Greenland ice sheet. *IEEE Transactions on Geoscience and Remote Sensing*, *50*(2), 585–592. https://doi.org/10.1109/TGRS.2011.2162072

Paterson, W. S. B. (1955). Altitudes on the inland ice of north Greenland. *Meddelelser om Grønland*, *137*(1), 1–12.

Patton, H., Swift, D. A., Clark, C. D., Livingstone, S. J., & Cook, S. J. (2016). Distribution and characteristics of overdeepenings beneath the Greenland and Antarctic ice sheets: Implications for overdeepening origin and evolution. *Quaternary Science Reviews*, *148*, 128–145. https://doi.org/10.1016/j.quascirev.2016.07.012

Peltier, W. R., Argus, D. F., & Drummond, R. (2015). Space geodesy constrains ice age terminal deglaciation: The global ICE-6G_C (VM5a) model. *Journal of Geophysical Research: Solid Earth*, *120*, 450–487. https://doi.org/10.1002/2014JB011176

Pilkington, M., & Grieve, R. A. F. (1992). The geophysical signature of terrestrial impact craters. *Reviews of Geophysics*, *30*(2), 161–181. https://doi.org/10.1029/92RG00192

Scambos, T. A., Haran, T. M., Fahnestock, M. A., Painter, T. H., & Bohlander, J. (2007). MODIS-based Mosaic of Antarctica (MOA): Continent-wide surface morphology and snow grain size. *Remote Sensing of Environment*, *111*(2-3), 242–257. https://doi.org/10.1016/j.rse.2006.12.020

Schaefer, J. M., Finkel, R. C., Balco, G., Alley, R. B., Caffee, M. W., Briner, J. P., et al. (2016). Greenland was nearly ice-free for extended periods during the Pleistocene. *Nature*, *540*(7632), 252–255. https://doi.org/10.1038/nature20146

Schmieder, M., Schwarz, W. H., Trieloff, M., Tohver, E., Buchner, E., Hopp, J., & Osinski, G. R. (2015). New $^{40}Ar/^{39}Ar$ dating of the Clearwater Lake impact structures (Québec, Canada)—Not the binary asteroid impact it seems? *Geochimica et Cosmochimica Acta*, *148*, 304–324. https://doi.org/10.1016/j.gca.2014.09.037

Schulte, P., Alegret, L., Arenillas, I., Arz, J. A., Barton, P. J., Bown, P. R., et al. (2010). The Chicxulub asteroid impact and mass extinction at the Cretaceous-Paleogene boundary. *Science*, *327*(5970), 1214–1218. https://doi.org/10.1126/science.1177265

Senft, L. E., & Stewart, S. T. (2008). Impact crater formation in icy layered terrains on Mars. *Meteoritics and Planetary Science*, *43*(12), 1993–2013. https://doi.org/10.1111/j.1945-5100.2008.tb00657.x

Studinger, M. (1998). Compilation and analysis of potential field data from the Weddell Sea, Antarctica: Implications for the breakup of Gondwana. *Reports on Polar Research*, *276*, 134.

Studinger, M. (2017). IceBridge ATM L2 Icessn elevation, slope, and roughness, version 2, NASA National Snow and Ice Data Center Distributed Active Archive Center, Boulder, Colorado. https://doi.org/10.5067/CPRXXK3F39RV. [Accessed 11 January 2016].

Tinto, K. (2018). IceBridge LDEO Gravimeter Suite L1B Geolocated Free Air Gravity Anomalies, Version 1. NASA National Snow and Ice Data Center Distributed Active Archive Center. https://doi.org/10.5067/SU3MNDAOQ7LZ. [Accessed 28 June 2018].

Walsh, K. J., & Jacobson, S. A. (2015). Formation and evolution of binary asteroids. In P. Michel, F. DeMeo, & W. F. Bottke (Eds.), *Asteroids IV*, (pp. 375–393). Tucson, AZ: U. Arizona Press. https://doi.org/10.2458/azu_uapress_9780816532131-ch020

Walsh, K. J., Richardson, D. C., & Michel, P. (2008). Rotational breakup as the origin of small binary asteroids. *Nature*, *454*(7201), 188–191. https://doi.org/10.1038/nature07078

Zwally, H. J., Giovinetto, M. B., Beckley M. A., & Saba, J. L. (2012). Antarctic and Greenland drainage systems. Available at: http://icesat4.gsfc.nasa.gov/cryo_data/ant_grn_drainage_systems.php

Erratum

The following corrections have been made to the originally published version of this article. Movie S2 has been replaced with an updated version; its caption remains unchanged. The title of the article as displayed in the Supporting Information S1 file has been corrected. Finally, the Kjær et al. (2018) reference has been updated with its published title. These errors have all since been corrected, and the present version may be considered the authoritative version of record.